

1 Supporting Information

2 Advancing Engineered Plant Living Materials  
3 through Tobacco BY-2 Cell Growth and  
4 Transfection within Tailored Granular Hydrogel  
5 Scaffolds

6 *Yujie Wang<sup>a</sup>, Zhengao Di<sup>b,c,\*</sup>, Minglang Qin<sup>a</sup>, Shenming Qu<sup>a</sup>, Wenbo Zhong<sup>a</sup>, Lingfeng Yuan<sup>a</sup>,*  
7 *Jing Zhang<sup>a</sup>, Julian M. Hibberd<sup>b</sup>, Ziyi Yu<sup>a,\*</sup>*

8 <sup>a</sup> State Key Laboratory of Materials-Oriented Chemical Engineering, College of Chemical  
9 Engineering, Nanjing Tech University, 30 Puzhu South Road, Nanjing 211816, P. R. China.

10 <sup>b</sup> Department of Plant Sciences, University of Cambridge, Downing Street, Cambridge CB2 3EA,  
11 UK.

12 <sup>c</sup> Earlham Institute, Norwich Research Park, Norwich, NR4 7UG, UK.

13 \* E-mail addresses: [ziyi.yu@njtech.edu.cn](mailto:ziyi.yu@njtech.edu.cn), [zhengao.di@earlham.ac.uk](mailto:zhengao.di@earlham.ac.uk) (Corresponding authors)

14  
15  
16  
17  
18  
19

20

21

22

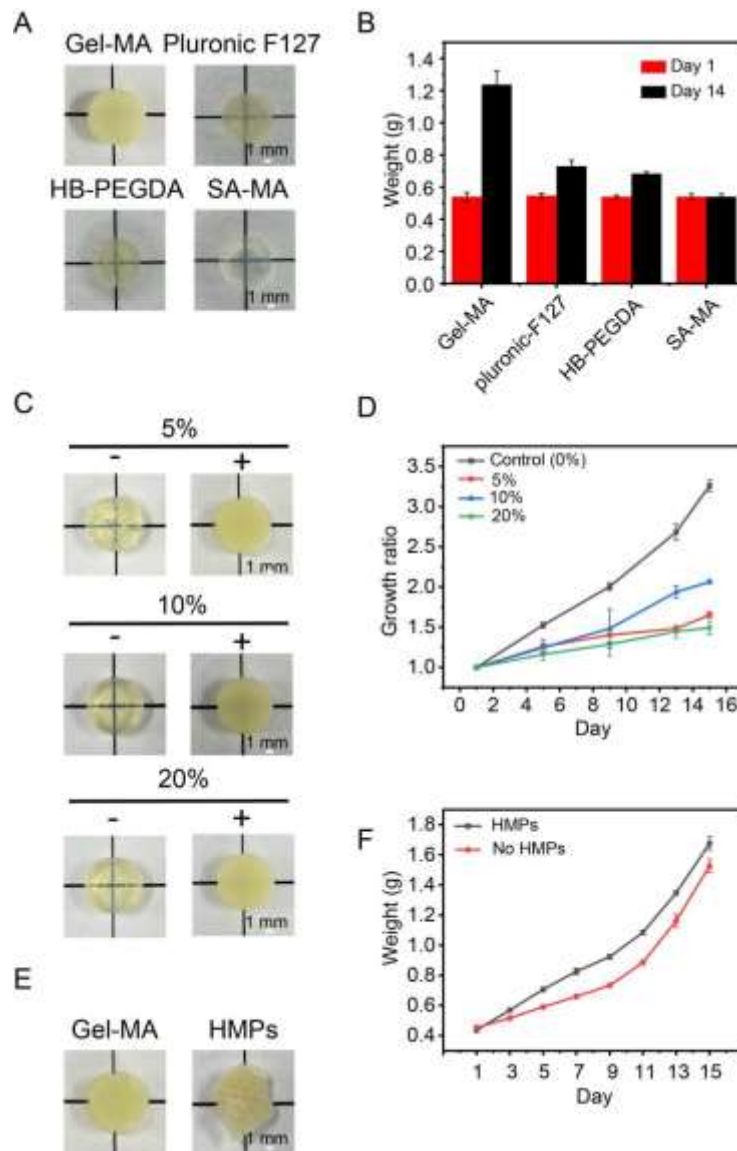
## Table of Contents

23

Figure S1:	Testing of different bioink materials for optimal plant cell growth.	1
Figure S2:	A microscopy image of generation of Gel-MA droplets by a microfluidic device.	2
Figure S3:	SEM images of hydrogel material.	3
Figure S4:	BY-2-loaded bioink for 3D printing.	4
Figure S5:	Rheological characterization of jammed BY-2 bioink.	5
Figure S6:	Optical and microscopy images of the growth of BY-2 within granular hydrogel scaffolds.	6
Figure S7:	Optical images showcasing the preservation of structural integrity and rigidity throughout the growth of PLMs.	7
Figure S8:	SEM and light microscopy images showing the presence of HMPs throughout the cultivation of BY-2 cells.	8
Figure S9:	Gel-MA hydrogel weight enlargement versus time.	9
Figure S10:	Optical and microscopy images of the growth of BY-2 cells at different locations of the scaffolds.	10
Figure S11:	Different shapes of PLMs fabricated by 3D bioprinting.	11
Figure S12:	Expression of GFP in BY-2 cells following <i>Agrobacterium</i> -mediated transformation.	12
Figure S13:	Effect of <i>Agrobacterium</i> inoculation time on BY-2 cells growth.	13
Figure S14:	Leakage and presence of <i>Agrobacterium</i> after inoculation.	14
FigureS15:	Contamination of BY-2 cells following <i>Agrobacterium</i> incubation.	15
FigureS16:	Schematic diagram and fluorescent image of suspension printed EPLMs, 14 days post-transformation.	16
FigureS17:	Transient expression of betalain biosynthetic pathway in <i>Nicotiana benthamiana</i> leaves following <i>Agrobacterium</i> -mediated infiltration.	17
FigureS18:	Growth of transformed and wild type PLMs.	18

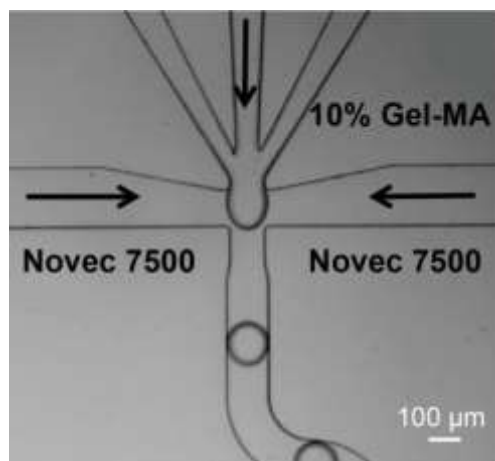
24

25



26  
 27 **Figure S1. Testing of different bioink materials for optimal plant cell growth.** A) Images  
 28 of BY-2-loaded materials consisting of Gel-MA, Pluronic F127, HB-PEGDA, or SA-MA (10%  
 29 wt) after 14 Days. Growth of BY-2 cells is indicated by the denser yellow color. B) Weights  
 30 of BY-2-loaded materials at day 1 and day 14. C) Images of different concentrations of  
 31 Gel-MA scaffolds with (+) or without (-) BY-2 cells 14 days after printing. D) Growth ratio  
 32 (total weight on certain dates divided by weight on the first day) of BY-2 cells in the presence  
 33 of different concentrations of Gel-MA. E) Images of scaffolds made by mixing BY-2 cells  
 34 with Gel-MA or HMPs after 14 days. F) Weight increases of BY-2 cells mixed in equal  
 35 volumes of HMPs or Gel-MA (No HMPs).

36



37

38 **Figure S2. A microscopy image of generation of Gel-MA droplets by a microfluidic**  
39 **device.**

40

41

42

43

44

45

46

47

48

49

50

51

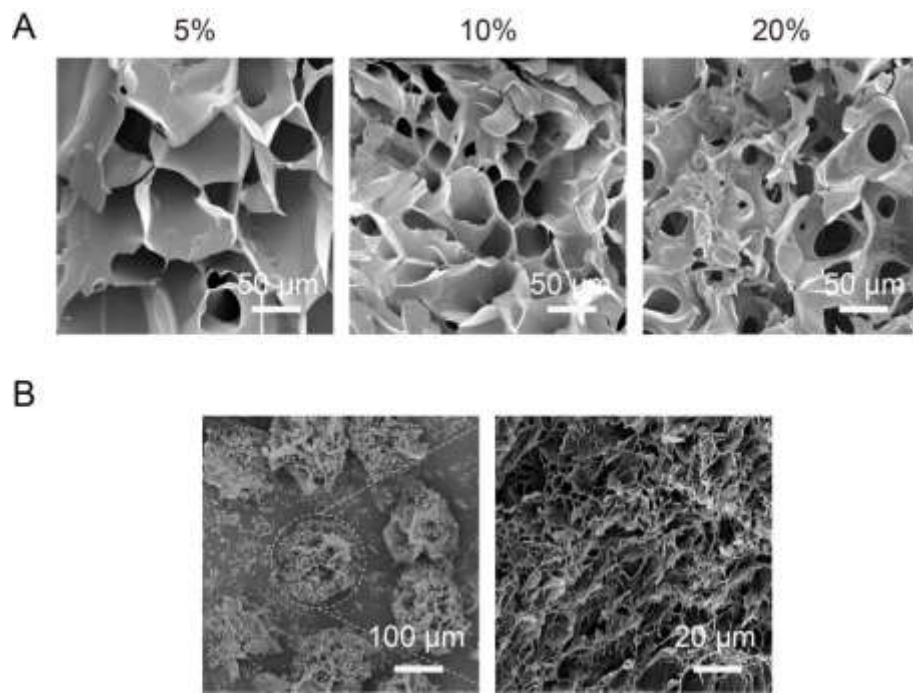
52

53

54

55

56



57

58 **Figure S3. SEM images of hydrogel material.** A) different Gel-MA concentrations. B)

59 HMP structures.

60

61

62

63

64

65

66

67

68

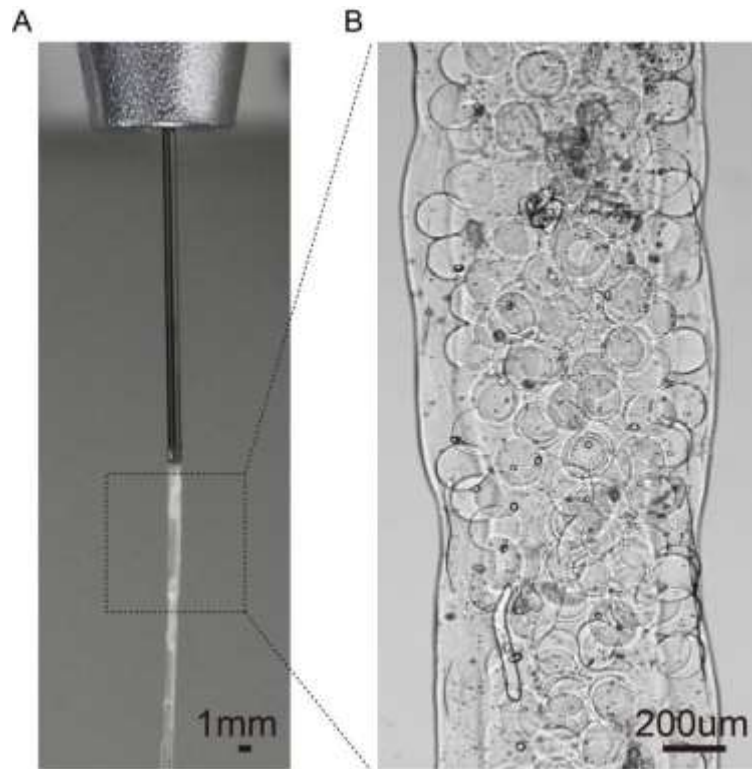
69

70

71

72

73



74

75 **Figure S4. BY-2-loaded bioink for 3D printing.** A) Images during jammed BY-2 bioink

76 extrusion. B) Microscopic image of jammed BY-2 bioink after extrusion.

77

78

79

80

81

82

83

84

85

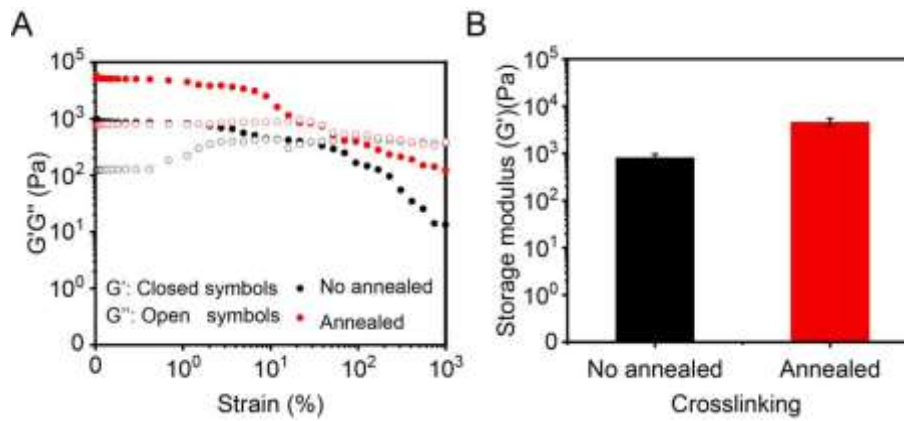
86

87

88

89

90



91

92 **Figure S5. Rheological characterization of jammed BY-2 bioink.** A) Storage moduli ( $G'$ )  
93 and loss moduli ( $G''$ ) of jammed BY-2 bioink. B) Storage modulus ( $G'$ ) of the granular  
94 hydrogels. Black and red colors represent jammed BY-2 bioink with and without annealing,  
95 respectively.

96

97

98

99

100

101

102

103

104

105

106

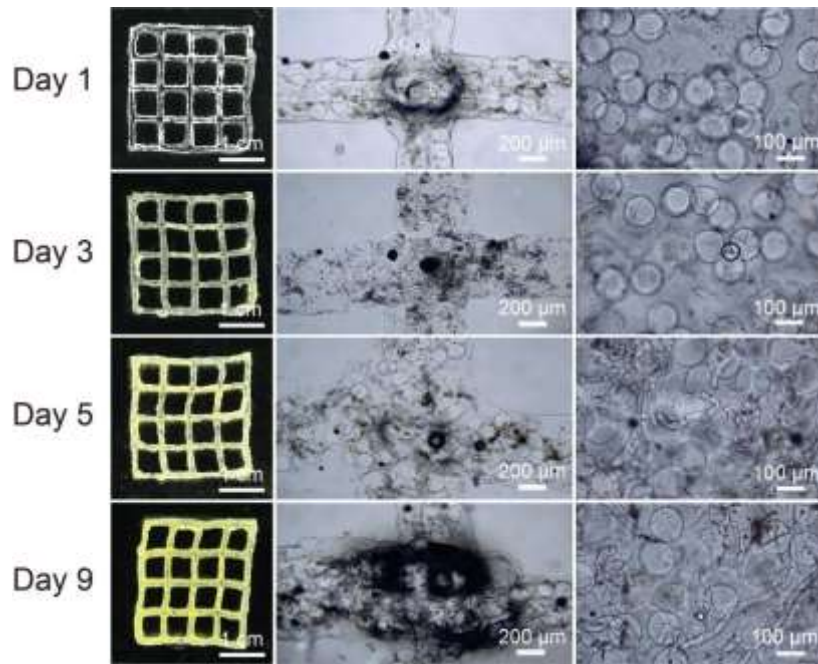
107

108

109

110

111



112

113 **Figure S6. Optical and microscopy images of the growth of BY-2 within granular**  
114 **hydrogel scaffolds.**

115

116

117

118

119

120

121

122

123

124

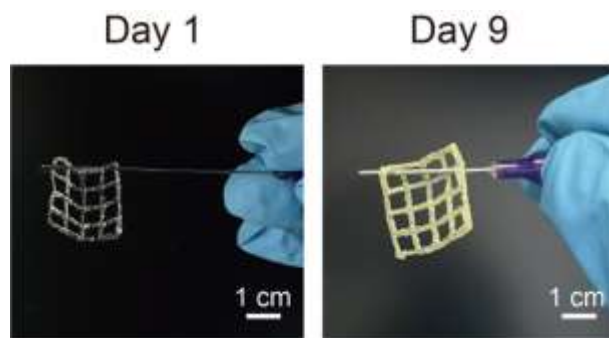
125

126

127



128



129

130 **Figure S7. Optical images showcasing the preservation of structural integrity and**  
131 **rigidity throughout the growth of PLMs.**

132

133

134

135

136

137

138

139

140

141

142

143

144

145

146

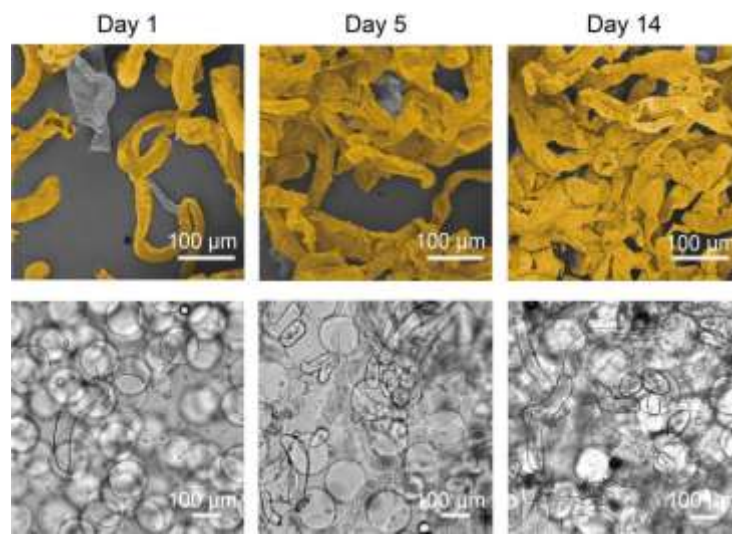
147

148

149

150

151



152

153 **Figure S8. SEM and light microscopy images showing the presence of HMPs throughout**  
154 **the cultivation of BY-2 cells.**

155

156

157

158

159

160

161

162

163

164

165

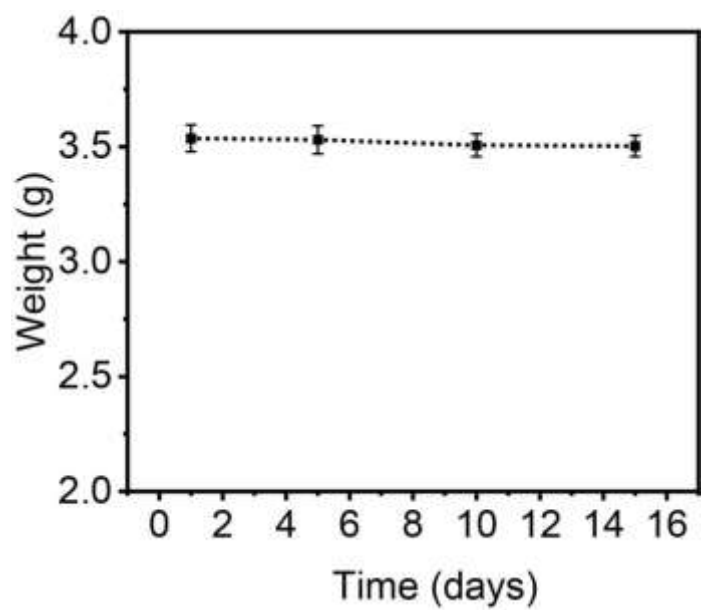
166

167

168

169

170



171

172

**Figure S9. Gel-MA hydrogel weight enlargement versus time.**

173

174

175

176

177

178

179

180

181

182

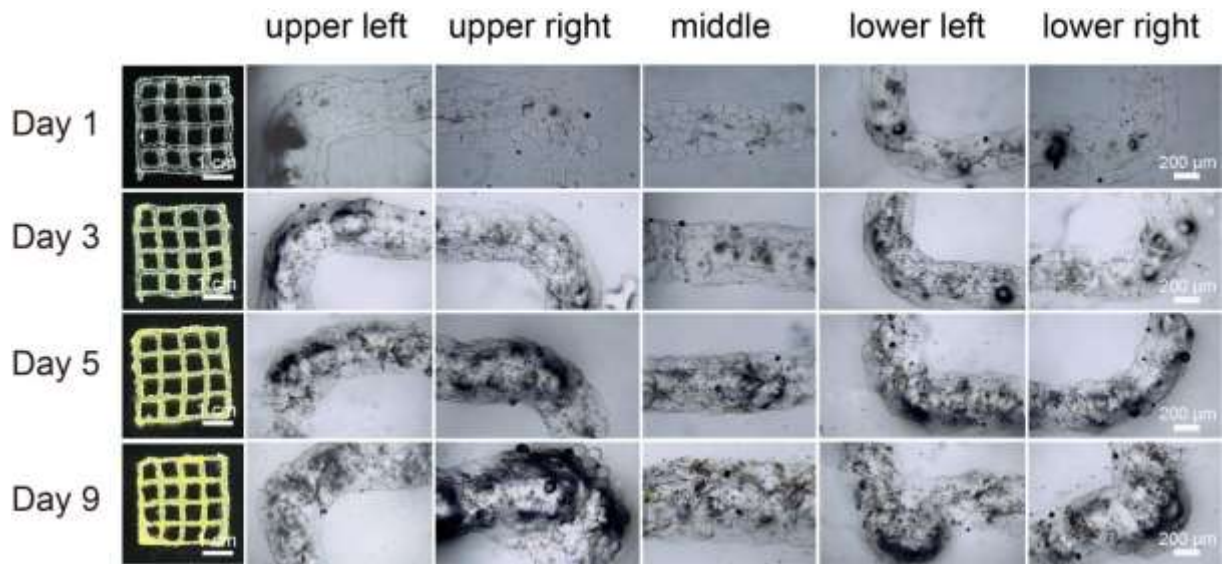
183

184

185

186

187



188

189 **Figure S10. Optical and microscopy images of the growth of BY-2 cells at different**  
 190 **locations of the scaffolds.**

191

192

193

194

195

196

197

198

199

200

201

202

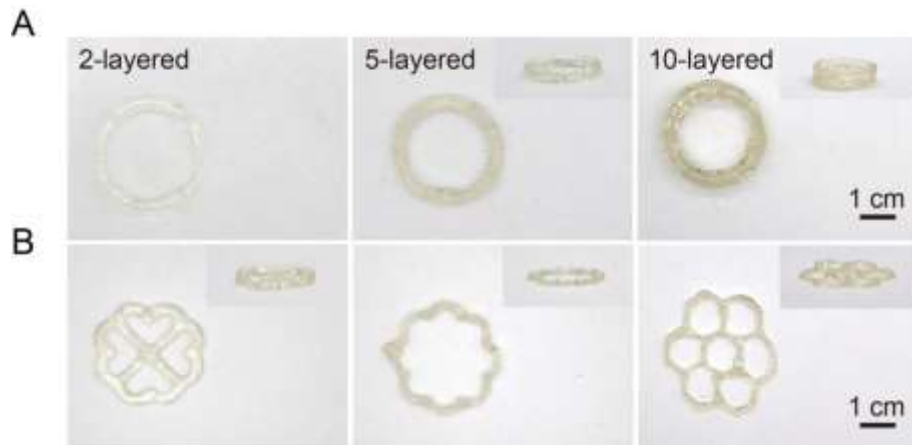
203

204

205

206

207



208

209 **Figure S11. Different shapes of PLMs fabricated by 3D bioprinting.** A) Side and top

210 views of multi-layer circular PLMs prepared by layer-by-layer deposition. B) Side and top

211 views of PLMs printed into various shapes.

212

213

214

215

216

217

218

219

220

221

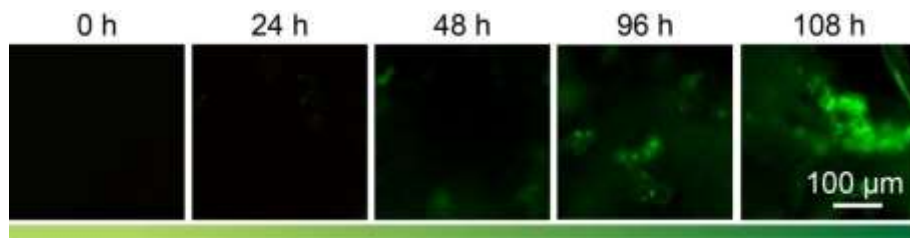
222

223

224

225

226



227

228 **Figure S12. Expression of GFP in BY-2 cells following *Agrobacterium*-mediated trans-**  
229 **formation.**

230

231

232

233

234

235

236

237

238

239

240

241

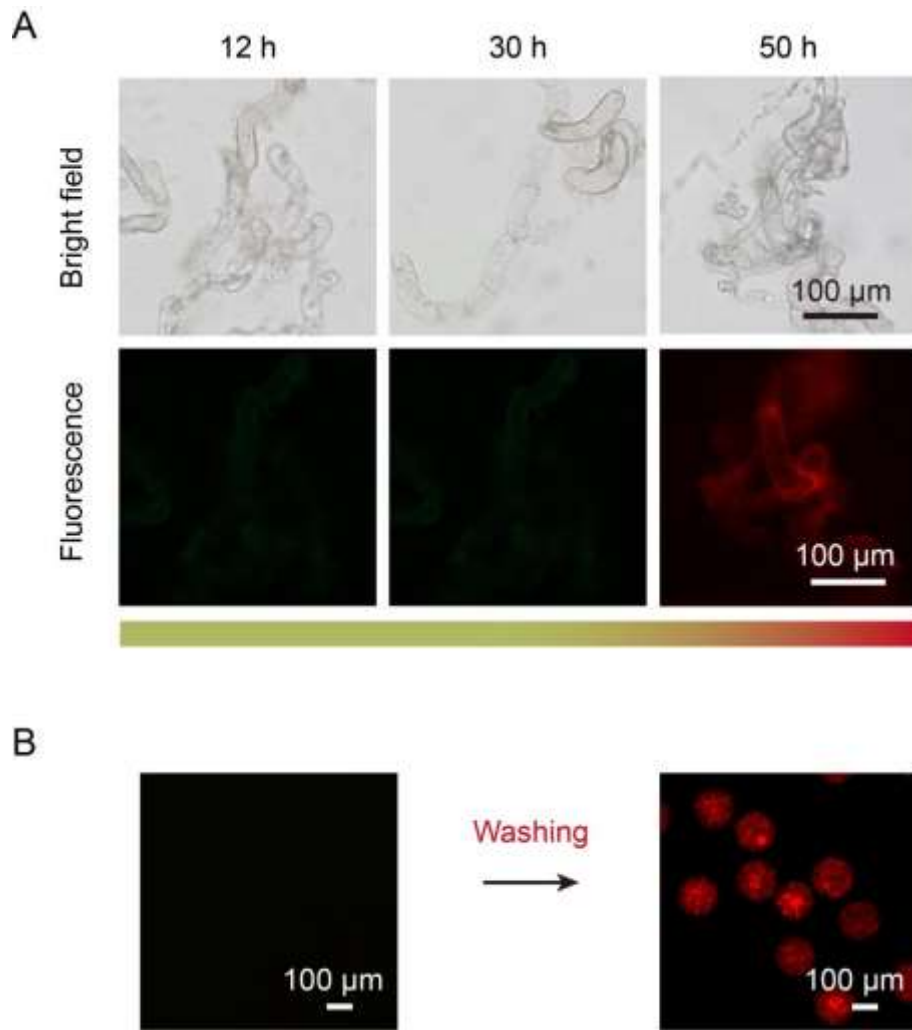
242

243

244

245

246



247

248 **Figure S13. Effect of *Agrobacterium* inoculation time on BY-2 cell growth.** A) Bright field

249 (top row) and fluorescence (bottom row) images of BY-2 cells following different hours of

250 *Agrobacterium* inoculation. Cells were stained ethidium homodimer-1 (EthD-1) and dead

251 cells appeared red. B) Fluorescence images of EthD-1 stained *Agrobacterium* embedded in

252 HMPs before and after washing in the MS media containing 25 μg/mL ampicillin.

253

254

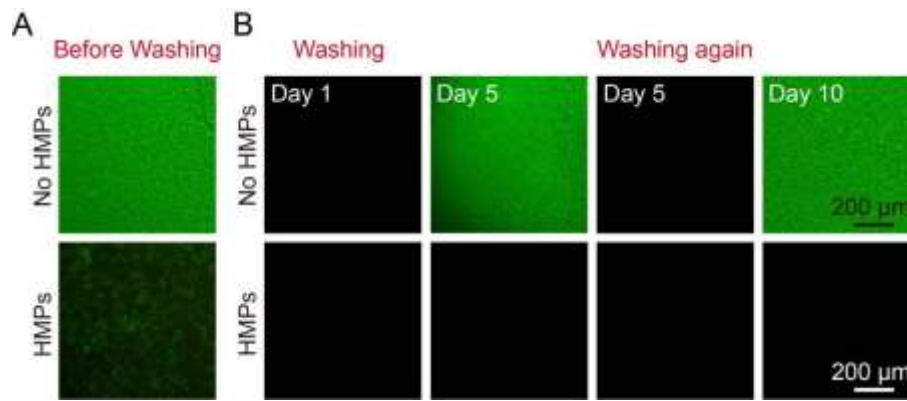
255

256

257

258

259



260

261 **Figure S14. Leakage and presence of *Agrobacterium* after inoculation.** No HMPs,  
 262 *Agrobacterium* culture was added directly to BY-2 callus growing on solid media. HMPs,  
 263 *Agrobacterium* were embedded in HMPs and mixed with BY-2 cells. A) After *Agrobacterium*  
 264 inoculation, BY-2 samples were soaped in fresh MS liquid media for 30 min, and  
 265 *Agrobacterium* leakage into the media visualized under fluorescence microscope. Cells were  
 266 stained with calcein acetoxymethyl (calcein AM) and live cells appeared green. B)  
 267 Transformed BY-2 cells were washed in MS media containing 25 μg/mL ampicillin and  
 268 grown for 5 days. Then BY-2 cells were soaped in MS liquid media and released  
 269 *Agrobacterium* observed under fluorescence microscope. C) The same washing-grow-soap  
 270 procedure was repeated. *Agrobacterium* could still be observed from BY-2 callus transformed  
 271 using traditional method (No HMPs) but not for HMP-mediated transformation method.

272

273

274

275

276

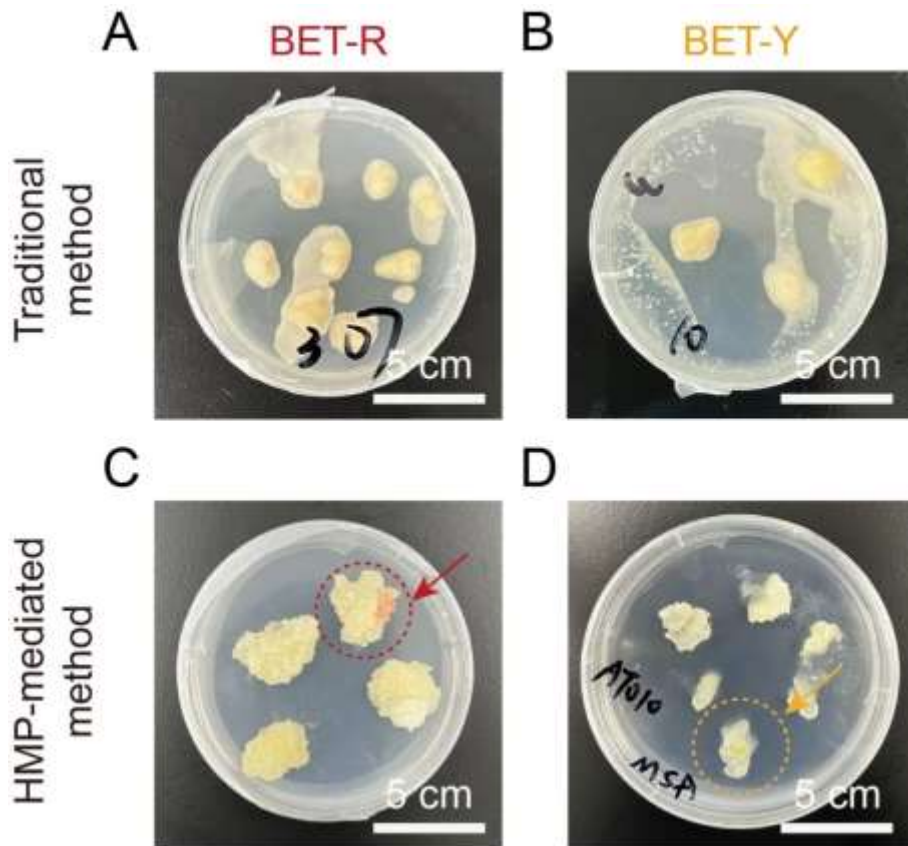
277

278

279

280

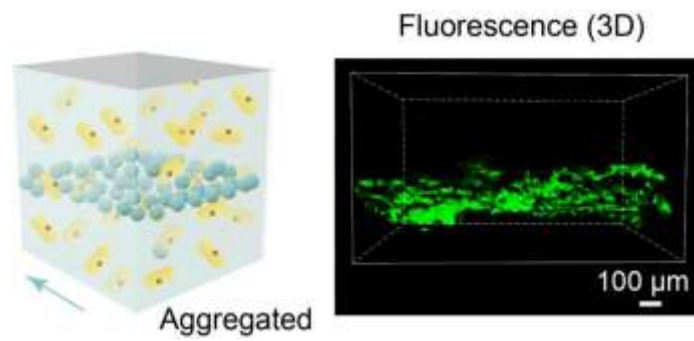




281  
 282 **Figure S15. Contamination of BY-2 cells following *Agrobacterium* incubation.** using  
 283 traditional (A, B) or HMP-mediated (C, D) transformation methods. BET-R (A, C) and  
 284 BET-Y (B, D) constructs were used and transformed cells showed red or yellow  
 285 pigmentations, respectively (highlighted by circles and arrows).

286  
 287  
 288  
 289  
 290  
 291  
 292  
 293  
 294  
 295

296



297

298 **Figure S16. Schematic diagram and fluorescent image of suspension printed EPLMs, 14**  
299 **days post-transformation.** *Agrobacterium*-loaded HMPs (blue spheres in the left schematic  
300 illustration) carrying GFP were printed into the central layer of a BY-2 cell culture chamber  
301 (yellow squares in the left schematic illustration).

302

303

304

305

306

307

308

309

310

311

312

313

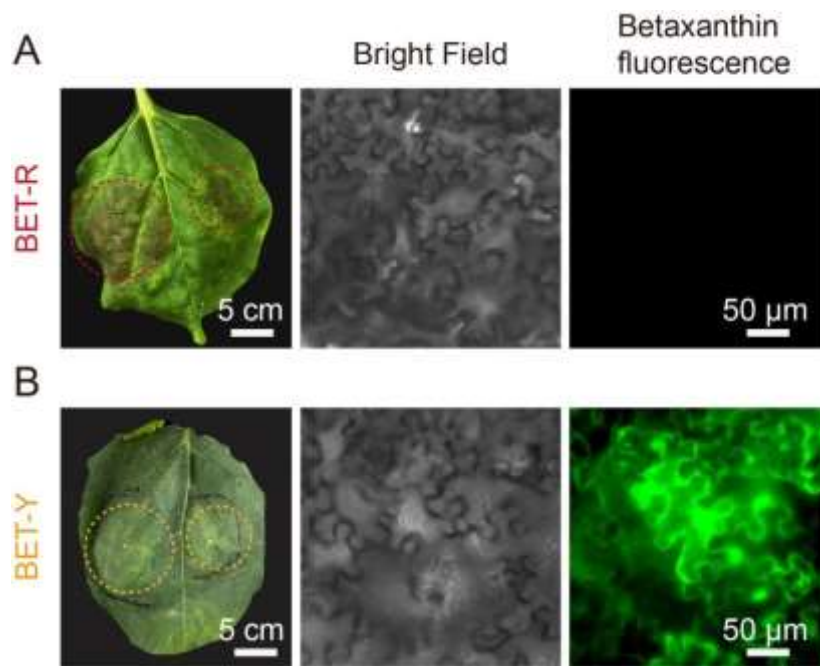
314

315

316

317

318



319

320 **Figure S17. Transient expression of betalain biosynthetic pathway in *Nicotiana***  
321 ***benthamiana* leaves following *Agrobacterium*-mediated infiltration. A-C) *N. benthamiana***  
322 **infiltrated with mixture of BET-R-1 and BET-R-2 *Agrobacterium* cultures (BET-R). A)**  
323 **Infiltrated area turned red. No betaxanthin fluorescence was observed under confocal**  
324 **microscope. B) *N. benthamiana* infiltrated with *Agrobacterium* culture carrying BET-Y**  
325 **construct. Infiltrated area turned slightly yellow, which was partly masked by the green color**  
326 **of the leaf and not clearly visible by the eye. Fluorescence corresponding to betaxanthin could**  
327 **be observed under confocal microscope.**

328

329

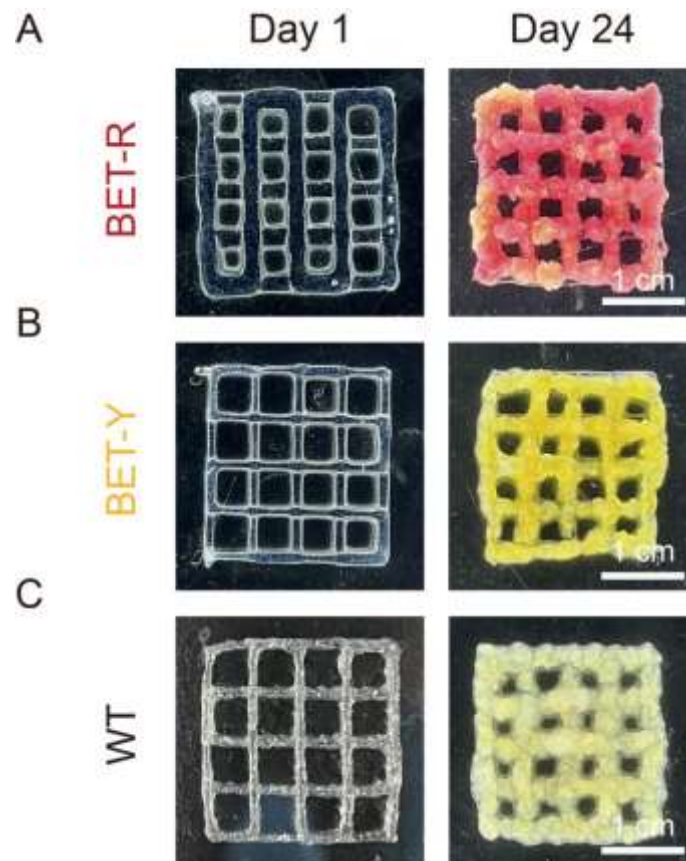
330

331

332

333

334



335

336 **Figure S18. Growth of transformed and wild type PLMs.** A) PLM printed from  
 337 BET-R-Ink. The lattice scaffold grew denser and turned red after 24 days due to betanin  
 338 production. B) PLM printed from BET-Y-Ink. The lattice scaffold grew denser and turned  
 339 yellow after 24 days due to betaxanthin production. C) PLM printed from bioinks containing  
 340 wild type *Agrobacterium*-loaded HMPs and BY-2 cells. The lattice scaffold grew denser and  
 341 turned slightly pale yellow, which was the same color as observed from BY-2 cells growing  
 342 in the liquid or solid MS media.

343

344

345

346

347

348